

# Steady-state humic-acid-containing blanket in upflow suspended bed

S.S. Sung<sup>a</sup>, D.J. Lee<sup>a,\*</sup>, Chihpin Huang<sup>b</sup>

<sup>a</sup>Chemical Engineering Department, National Taiwan University, Taipei 10617, Taiwan

<sup>b</sup>Institute of Environmental Engineering, National Chiao Tung University, Hsinchu 300, Taiwan

Received 1 July 2004; received in revised form 2 December 2004; accepted 7 December 2004

## Abstract

We investigated the effects of turbidity and concentration of humic acid on the steady-state behavior of the blanket, which was coagulated using polyaluminum chloride (PACl) as coagulant. The three-dimensional solid-flux plot was constructed. Based on fixed PACl dosage, the iso-humic-acid solid-flux surfaces stacked that enveloped the feasible regime for the blanket bed. The steady-state point moved toward low solid flux and low solid fraction regime with decreasing initial raw water turbidity and/or increasing humic-acid concentration. Low water turbidity and high humic-acid concentration yielded a bulky blanket, with the former producing clean, and the latter turbid effluent. The presence of humic acid was thereby harmful to blanket strength, except for the case of low raw water turbidity. An optimal range of humic acid for blanket strength and clarification efficiency existed at  $1 \text{ mg l}^{-1}$ . Low level of humic acid is beneficial to blanket development with low-turbidity raw water.

© 2005 Elsevier Ltd. All rights reserved.

*Keywords:* Flocculation clarifier; Blanket; Stability; Humic acid; Drinking water

## 1. Introduction

Flocculation clarifier provides more efficient coagulation of suspended particles, thereby yielding a surface loading two to three times higher than conventional coagulation–sedimentation basin (Kawamura, 1991; Masschelein, 1992; Stevenson, 1997; Edzwald et al., 1999). The floc blanket acts as both a particle coagulator and a filter, and thus is essential for clarifiers to produce quality drinking water (Gregory et al., 1996; Head et al., 1997). Stringent operational control is required to prevent sludge washout from the clarifiers (AWWA/ASCE, 1990).

Ives (1968) proposed a model for particle removal in the clarifier. This model nonetheless overestimated the particle removal efficiency of the clarifier and predicted an unrealistic solid concentration distribution in the blanket. Could (1974) modeled the blanket by assuming that the change in blanket height is controlled by the upflow velocity and the settling velocity. Based on Could's model, Head et al. (1997) modeled the removal of particle entering the blanket by applying the solid-flux theory by Could. Head et al.'s model assumed a completely mixed blanket. As Sung et al. (2003) reported, when blanket carryover occurred at the reduction in coagulant dose, a concentration "wave" emerged from the tank bottom and moved upward.

Chen et al. (2003) proposed the simplified, one-dimensional model for the spatio-temporal variation of solids fraction in the blanket considering both the

\*Corresponding author. Tel.: +886 2 2362 5632;

fax: +886 2 2362 3040.

E-mail address: djlee@ccms.ntu.edu.tw (D.J. Lee).

hydrodynamic dispersion and the convection effects as follows:

$$\frac{\partial C}{\partial t} = D \frac{\partial^2 C}{\partial z^2} - \frac{\partial C\{U - V_{\text{sett}}(C, \text{AVI}, d_f, \dots)\}}{\partial z}, \quad (1)$$

where  $C$  (-) is the solid fraction,  $D$  ( $\text{m}^2$ ) the effective diffusivity of flocs in the blanket,  $U$  the upflow velocity ( $\text{mh}^{-1}$ ),  $V_{\text{sett}}$  the local settling velocity ( $\text{mh}^{-1}$ ), AVI the floc volume (%), and  $t$  (h) the process time. Field observation normally revealed a rather uniform distribution of solid fraction in the floc blanket (Head et al., 1997). In addition, at steady-state operation, the blanket surface presented as a distinct surface from the clear supernatant. Hence, the steady-state blanket concentration,  $C_s$ , could be obtained by solving

$$C_s U - C_s V_{\text{sett}}(C_s, \text{AVI}, d_f, \dots) = 0. \quad (2)$$

Restated, by equating the solid-fluxed  $CU$  and  $CV_{\text{sett}}$ , the steady-state  $C_s$  could be found graphically.

Based on experimental observation, Su et al. (2004) utilized the simplified one-dimensional model for exploring the dynamic characteristics of the blanket in a fluidized bed. Experiments with synthetic raw water coagulated with PACl were conducted to verify their theoretical findings. Briefly, at  $D = 0$  limit, the no-dispersion approximation, Eq. (1) becomes a wave equation as follows:

$$\frac{\partial C}{\partial t} + \left\{ \frac{\partial(C(U - V_{\text{sett}}(C)))}{\partial C} \right\} \frac{\partial C}{\partial z} = \frac{\partial C}{\partial t} + v(C) \frac{\partial C}{\partial z} = 0, \quad (3)$$

which has a shock-wave solution with  $v(C)$  ( $\text{mh}^{-1}$ ) being the characteristic velocity.

Fig. 1 shows the schematics of the solid-flux curves (Su et al., 2004). According to Eq. (3), regardless of the shape of the initial distribution, the solid fraction in the

blanket would converge to a shock wave-like solution at  $C = C_0$ . That is,  $C$  within the blanket is uniformly distributed above in which the supernatant existed with  $C \sim 0$ . To balance the mass in the blanket, subsequently, the blanket would evolve to another shock wave solution at  $C = C_s$  (Fig. 1), determined by the intersection of  $CU$  and  $CV_{\text{sett}}$  curves. Disturbance always occurred in the blanket, such as the change in raw water quality or that in coagulant dose. The blanket afterward evolved with time, with how fast the blanket would approach the steady-state distribution determined by Eq. (3). The solid-flux plots together with the so-called “critical velocity”,  $U_{\text{crit}} = \lim_{C \rightarrow 0} (\partial(CV_{\text{sett}})/\partial C)$  ( $\text{ms}^{-1}$ ), are essential for realizing the blanket dynamics. At  $U > U_{\text{crit}}$  there would be no steady-state solution of  $C$ , indicating complete loss of blanket.

Humic substances commonly presented in the raw water of Taiwan, particularly after heavy showers that brought in highly turbid raw water (Annadurai et al., 2003). Mechanisms corresponding to the coagulation removal of organic substances had been discussed (Dempsey et al., 1984; Dempsey, 1989; O’Melia, 1991). Narkis and Rebhun (1990) showed that when both mineral particles and dissolved humic substances are present in raw water, the latter controls the coagulation process. Coagulation of humic-substance-containing suspension would produce highly turbid supernatant (Tambo and Watanabe, 1979; Rebhun, 1990). However, how the levels of mineral particles and of humic acid affect the blanket behavior remains unclear. We investigated in this work the effects of turbidity and concentration of humic acid on the blanket stability, evaluated by recording blanket behavior subjected to different upflow velocities. The critical velocity and the maximum velocity corresponding to  $C = C_{\text{max}}$  were identified. A three-dimensional solid-flux plot was constructed to demonstrate the role of humic acid and water turbidity on steady-state blanket.

## 2. Experimental

The synthetic raw water was prepared by mixing a prescribed amount of UK ball clay powders and  $10^{-2}$  N  $\text{NaClO}_4$  solution to a solids content of  $62.5\text{--}1000 \text{ g l}^{-1}$ , giving a turbidity of  $40\text{--}1000 \text{ NTU}$ . The suspension alkalinity was adjusted by adding  $\text{NaHCO}_3$  salt to  $100 \text{ mg l}^{-1}$  equivalent. The pH was adjusted at 7.0 using  $\text{HClO}_4$  and  $\text{NaOH}$ . Humic acid with a carbon content of 52.6% was purchased from the International Humic Substances Society (IHSS). The stock solution of humic acid was made by first dissolving the chemicals in a solution at pH 12. After filtering with a  $0.45 \mu\text{m}$  cellulose nitrate membrane, the pH of filtrate was adjusted back to 7.0. The humic acid was dosed at the prescribed amount and mixed with the clay suspension overnight

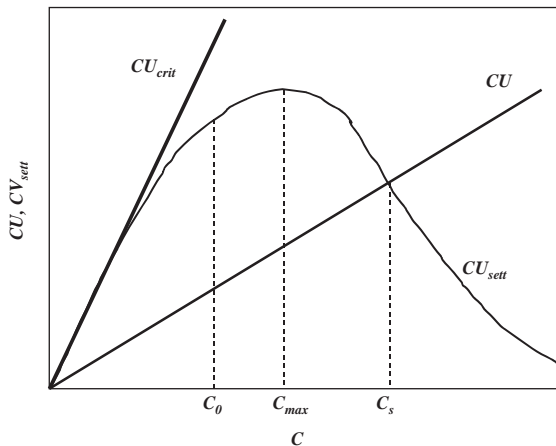


Fig. 1. Solid-flux plot for upflow suspension bed.  $C_0$  is the solid fraction at which spatial derivative of  $(CU - CV_{\text{sett}})$  vanishes.

Table 1  
Experimental conditions and the legend used

Turbidity (NTU)	Humic acid ( $\text{mg l}^{-1}$ )			
	0	1	3	7
40	#1	#2	#3	#4
100	#5	#6	#7	#8
200	#9	#10	#11	#12
1000	#13	#14	#15	#16

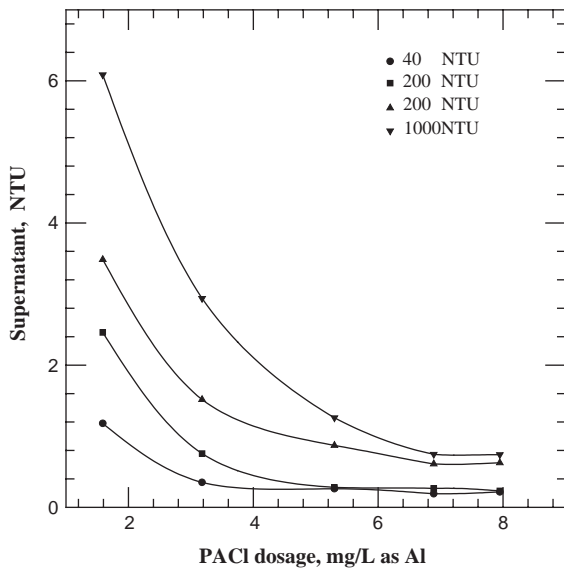


Fig. 2. Residual turbidity of coagulated water after 2-h settling.

before use. Table 1 lists the legends for the experimental conditions adopted.

The suspension was coagulated in a jar tester. The  $1000 \text{ mg l}^{-1}$  PACI solution, with 11% available  $\text{Al}_2\text{O}_3$ , was slowly injected into the stirred suspension at 90 rpm for 1.5 min, and then at 50 rpm for 8.5 min. Fig. 2 shows the supernatant turbidity of coagulated water after 2-h settling. On this plot the optimal dose for 100-NTU raw water was estimated,  $5.3 \text{ mg l}^{-1}$  as Al. To demonstrate the effects of presence of humic acid and of initial turbidity of raw water, the PAC dose was fixed at  $5.3 \text{ mg l}^{-1}$  as Al in this work.

The sediment of the coagulated raw water was carefully collected, and was gradually poured into a cylindrical column of diameter 5.7 cm and of height 87 cm with care. A low upflow velocity was applied continuously from the column bottom during the sediment pouring. Su et al. (2004) revealed that this low upflow velocity was essential to keep the sediment in a suspended state for getting reproducible data since the compaction of sediment at the column bottom would

yield irreversible change in its structure (Chu and Lee, 2001; Chu et al., 2002a, b).

The equilibrium heights of blanket interface were recorded at various upflow velocities. A turbidimeter (HACH Model 2100 AN) measured the turbidities of the effluent from the fluidized bed.

### 3. Results and discussion

#### 3.1. Blanket behavior

Fig. 3 shows the blanket dynamics for test #4, with coagulated sediment with low clay content and high humic-acid concentration ( $7 \text{ mg l}^{-1}$ ). At  $U = 1.1 \text{ m h}^{-1}$ , the blanket stably existed at a height of 5.5 cm with clear interface (Fig. 4a) and supernatant turbidity of 6 NTU. At  $U = 2.2 \text{ m h}^{-1}$ , the interface of the blanket was still distinguishable (Fig. 3), with its height increased to 16 cm. The corresponding supernatant turbidity was 12 NTU. Further increase in  $U$  to  $2.6 \text{ m h}^{-1}$  resulted in, small flocs being carried upward from the clarifier, with interface becoming blurred (Fig. 3). The blanket height was 22 cm and the supernatant turbidity was 15 NTU. Complete blanket loss occurred at  $U > 2.6 \text{ m h}^{-1}$ . Fig. 3 also reveals the case with  $U = 4.0 \text{ m h}^{-1}$ , showing a conveying bed characteristic. The critical velocity of the blanket in test #4 was as estimated 2.6 m/hr.

Fig. 4 also shows the blanket heights for tests #1–#3. Apparently, with humic acid  $< 1 \text{ mg l}^{-1}$ , the blanket was compact in structure, leading to a low blanket height. For instance, for tests #1 and #2, the blanket height was only 2.5 and 4.5 cm at  $U = 1.1$  and  $2.2 \text{ m h}^{-1}$ , respectively. The corresponding supernatant turbidities were 3.5 and 4 NTU, respectively. The critical velocities were  $4.5 \text{ m h}^{-1}$  for test #1, and  $4.7 \text{ m h}^{-1}$  for test #2. On the other hand, test #3, with humic acid of  $5 \text{ mg l}^{-1}$ , had dynamic characteristics resembling those of test #4.

Fig. 4b shows the solid-flux plots for tests #1–#4 and the contours of upflow velocities. The solid flux revealed an increasing–decreasing characteristic, with  $C_{\text{max}} = 1.0\%$  and  $0.71\%$  for tests #1 and #2, and #3 and #4, respectively. The corresponding maximum solid fluxes were  $2.1 \text{ wt\% m h}^{-1}$  and  $0.92 \text{ wt\% m h}^{-1}$ , presenting a relatively low solid flux. With a low raw water turbidity of 40 NTU, overdosing in PACI led to a loosely structured blanket, while the presence of humic acid in greater amounts than  $3 \text{ mg l}^{-1}$  assisted in making an even more bulky blanket.

Fig. 5 shows the blanket dynamics for test #16, with coagulated sediment with both high initial turbidity (1000 NTU) and high humic-acid concentration ( $7 \text{ mg l}^{-1}$ ). At  $U = 2.0 \text{ m h}^{-1}$ , the blanket stably existed at a height of 12 cm with blurred interface (Fig. 6a) and supernatant turbidity of 96 NTU. At  $U = 2.8 \text{ m h}^{-1}$ , the interface of the blanket was not distinguishable (Fig. 5),

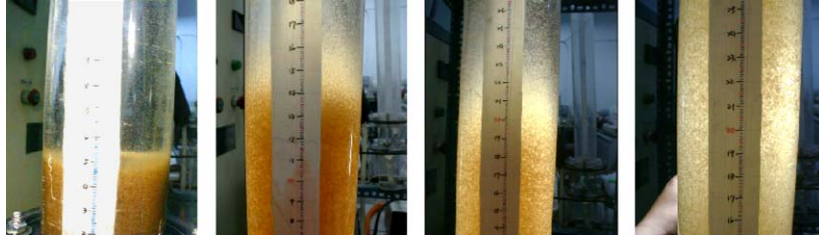


Fig. 3. Blanket behavior at various upflow velocities. Test #4. (Left to right):  $U = 1.1, 2.2, 2.6, 4.0 \text{ m/h}$ .

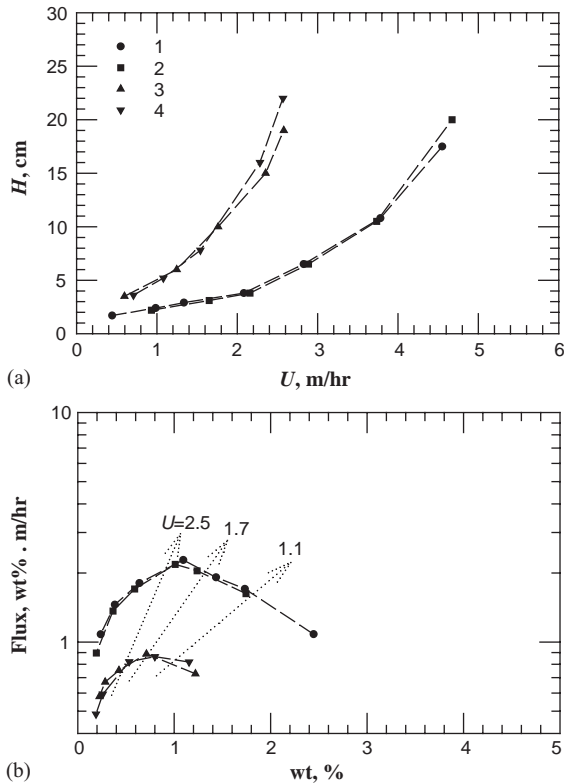


Fig. 4. Experimental results #1–4. Initial turbidity of water to make a blanket = 40 NTU. (a) Blanket height versus upflow velocity plot; (b) solid flux versus solid concentration plot.

with its height increased to 20 cm. The corresponding supernatant turbidity was still around 100 NTU. Further increase in  $U$  led to sludge carryover. Hence, both high clay and humic-acid concentrations probably underdosed the coagulation, leading to poorly developed networks among particles. The blanket was easily expanded under upflow, and easily eroded to yield high turbidity in supernatant.

Fig. 6b shows the solid-flux plots for tests #13–#16 and the contours of upflow velocities. The solid flux revealed an increasing–decreasing characteristic, with  $C_{\max} = 5.4\%$ ,  $4.3\%$ ,  $2.5\%$ , and  $2.2\%$  for tests #13–#16, respectively.

With high clay concentration, the stability of the coagulated blanket still deteriorated with humic acid, but with less influence as revealed in tests #1–#4. Insufficient coagulation yielded turbid supernatant, and a less effect of humic acid on the network of coagulated particles.

Tests #5–#12 are not shown here for brevity. The corresponding solid-flux curves located among those are shown in Figs. 4 and 6.

### 3.2. Characteristic velocities

On each solid-flux curve, the straight line of  $CU_{\text{crit}}$  represents the asymptotic behavior of the solids flux at  $C \rightarrow 0$  limit, which was used to bound the left margin of the solid-flux curve. Theoretically one could operate this blanket up to  $U_{\text{crit}}$ . However, as experiments revealed, the blanket interface became blurred at an upflow velocity lower than  $U_{\text{crit}}$ . Without theoretical justification, Gregory et al. (1996) recommended to operate the blanket at  $C = C_{\max}$  based on field observation. Since  $U_{\max} < U_{\text{crit}}$ , Gregory's proposal could be used as a convenient index in the operation.

Fig. 7 shows the  $U_{\max}$  and  $U_{\text{crit}}$  data for the 16 mentioned tests. Except for test #2, the two characteristic velocities decreased linearly with increasing humic-acid/clay concentration ratio. The blanket with higher characteristic velocities exhibits a network of higher strength. Therefore, the presence of humic acid would deteriorate the blanket structure, while that of clay particles would strengthen it. In addition, the universal correlation noted in Fig. 7 shows that the humic-acid/clay concentration ratio is an essential factor that controls the blanket stability.

### 3.3. Solid-flux plot

Fig. 8 shows the three-dimensional solid-flux plot summarizing the results of tests #1–#16. The critical velocity became a  $CU = CU_{\text{crit}}$  plane in the figure, to the left of which the blanket could not stably exist. Based on fixed PACl dosage, the iso-humic-acid solid-flux surfaces stacked that enveloped the feasible regime for the blanket. Each point on the surface represented a steady-state operation of the blanket; hence, based on

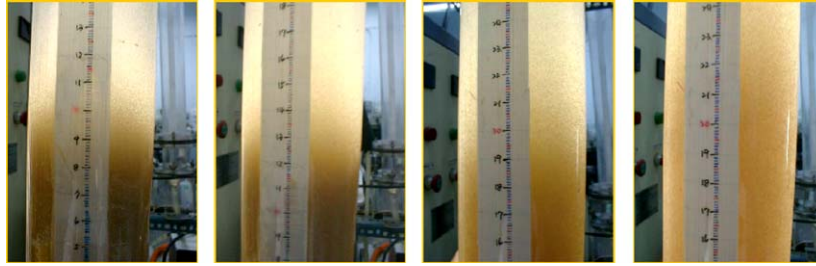


Fig. 5. Blanket behavior at various upflow velocities. Test #16. (left to right):  $U = 2.0, 2.2, 2.8, 4.0 \text{ m/h}^{-1}$ .

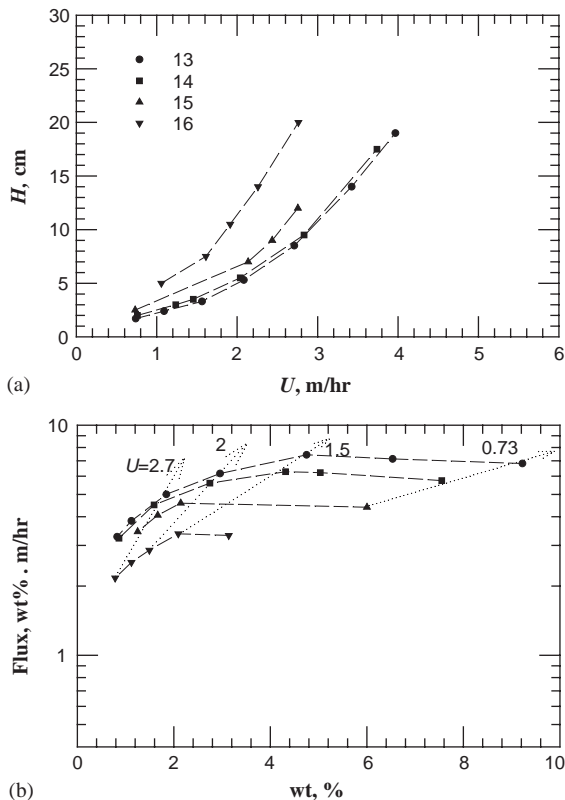


Fig. 6. Experimental results #13–16. Initial turbidity of water to make a blanket = 1000 NTU. (a) Blanket height versus upflow velocity plot; (b) solid flux versus solid concentration in blanket plot.

this 3D plot, the blanket behavior could be realized. The steady-state point moved toward low solid flux and low  $C_s$  regime with decreasing initial raw water turbidity and/or increasing humic-acid concentration. Nonetheless, although the characteristic velocities shown in Fig. 7 could be correlated with the humic-acid/clay concentration ratio, the solid-flux surfaces shown in Fig. 8 could not be easily described by a universal surface by simply adopting the concentration ratio

instead of the raw water turbidity as independent parameter.

Fig. 8 could be used to control the blanket dynamics. As revealed in Su et al. (2004) once an originally stable blanket was “disturbed”, by change in raw water quality, PACl dose, start-up, shut-down, etc., the blanket concentration profile would first evolve to a shock wave-like distribution of  $C = C_{\max}$ . Afterward, it would compact to another shock-wave distribution of  $C = C_s$ . The blanket concentration presents an important process parameter determining its capability to screen off coagulated particles (Gregory, 1979). However, the present study revealed that the blanket concentration is a strong function of raw water turbidity and humic-acid concentration, and is not an adequate performance index subjected to a wide range of raw water quality.

### 3.4. Blanket clarification

With high raw water turbidity, the dosed coagulant was insufficient for satisfactory coagulation; consequently, the blanket was not fully developed under upflow and presented a compact sediment layer at the column’s bottom. The corresponding effluent turbidity was high while the blanket presented no active role to particle coagulation and catchments. At low raw water turbidity the present coagulant was overdosed, leading to a bulky blanket structure. A bulky blanket was noted beneficial to particle coagulation and capture in a previous investigation (Su et al., 2004). However, the humic acid would compete for fine particles in suspension with the available coagulant (Rebhun and Lurie, 1993). Since the blanket deteriorated in structural networks due to humic acid, the produced blanket was also bulky, with its effluent high in turbidity. At a high humic-acid concentration, the blanket itself easily eroded by upflow to produce small pieces of flocs that contributed to effluent turbidity. Therefore, a bulky blanket is not always beneficial to particle removal.

As mentioned above, the suspensions with either none or high humic acid were not ideal candidates for producing the “ideal” blanket, not loose enough in

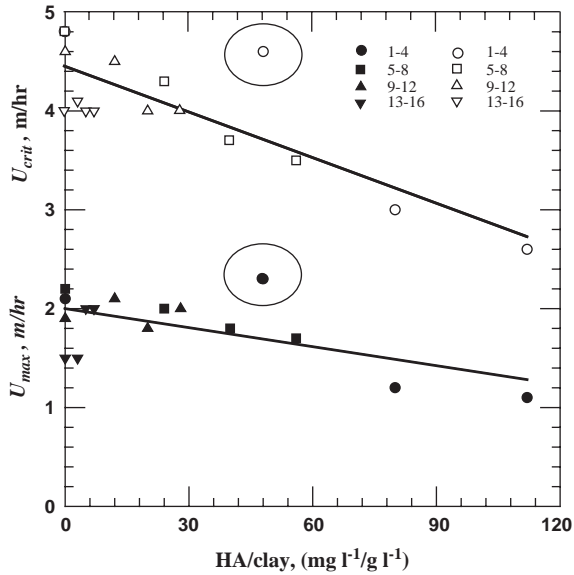


Fig. 7.  $U_{max}$  and  $U_{crit}$  as functions of ratio of humic-acid concentration and clay content to make the blanket.

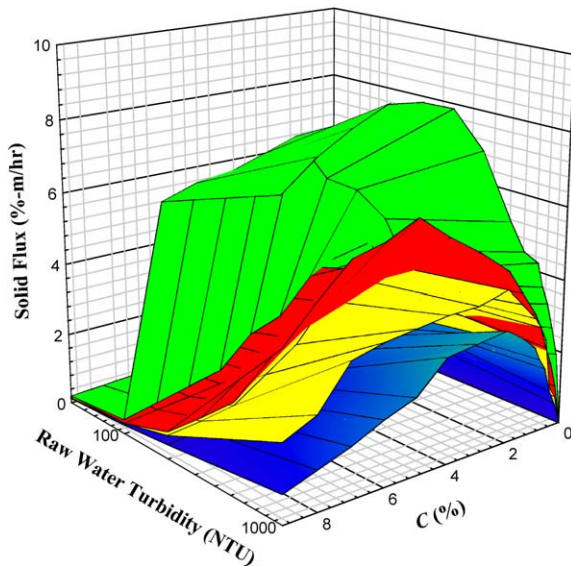


Fig. 8. Three-dimensional solid-flux plot for steady-state blankets. Top to bottom: humic-acid concentration = 0, 1, 5, and 7 ppm.

structure to allow satisfactory particle coagulation and catchments, and also not tough enough in strength to prevent floc erosion by upflow. There possibly existed an “optimal” concentration range of humic acid with which the ideal blanket could be satisfactorily developed. The characteristic velocities of test #2, circled in Fig. 7, were

higher than that expected from the trend lines. With  $1 \text{ mg l}^{-1}$  humic acid, the blanket produced by coagulation of low-turbidity raw water would therefore have higher structural strength than those without or with more humic acid. Fig. 9 shows the microphotographs of the floc appearance produced by different levels of humic acid. The flocs by  $1 \text{ mg l}^{-1}$  humic acid were larger in size than those without or with high levels of humic acid.

O’Melia (2004) recently noted that the coagulant dose would be much less than expected to satisfactorily coagulate low-turbidity water if a small amount of organic substance was present (O’Melia, 2004). However, organic substance could not assist coagulation when the water turbidity was high.

To demonstrate the efficiency of particle clarification, the blankets produced by tests #1–#4 were placed in the upflow bed, through which a synthetic raw water stream was allowed to flow. The influent raw water was made at pH 7.0 and  $10^{-2} \text{ N NaClO}_4$ , with clay suspension, to reach turbidities of 40 or 450 NTU and PACl dosed at  $5.3 \text{ mg l}^{-1}$  as Al. The effluent was sampled, whose turbidities are shown in Fig. 10.

The blanket had better clarification efficiency when 1-ppm humic acid was present during blanket generation. With higher humic-acid content, the produced blanket failed to satisfactorily clarify the coagulated water stream. In fact, at a humic-acid concentration of  $7 \text{ mg l}^{-1}$ , the effluent turbidity was even higher than the influent turbidity (40 NTU), indicating that part of the blanket was eroded upstream that yielded more turbidity than the incoming stream. Hence, an optimal range of humic acid does exist for yielding an ideal blanket.

#### 4. Conclusions

We coagulated the humic-acid-containing clay suspension using polyaluminum chloride (PACl) as coagulant, and recorded the steady-state blanket behavior in an upflow bed. At prescribed upflow velocity, the blanket would have a loose structure when the suspension to produce the blanket was of low-turbidity and/or of high humic-acid content. Based on the one-dimensional model by Su et al. (2004) the solid-flux curve and the critical upflow velocity were identified for various blankets.

When raw water turbidity was high, the blanket was compact in structure with insufficient PACl dose. The corresponding solid flux was high. With low water turbidity, on the other hand, the blanket was bulky and yielded low effluent turbidity. With high humic-acid concentration, the blanket was deteriorated in structure and also led to a bulky structure. However, the corresponding effluent turbidity was high. A bulky

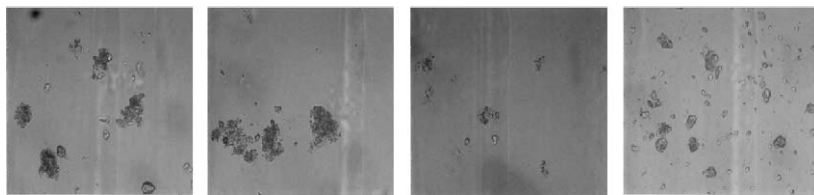


Fig. 9. Microphotographs of the coagulated flocs. PACl 5.3 ppm as Al. Initial raw water turbidity = 40 NTU. (left to right): Humic acid concentration = 0, 1, 3, 7 ppm.

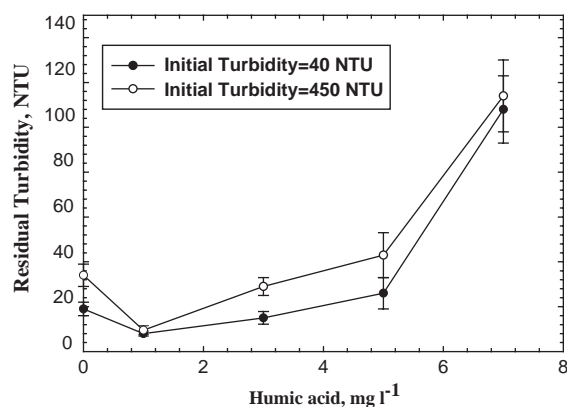


Fig. 10. Residual turbidity of effluent with influent stream of 40 or 450 NTU flowing through the blanket (produced by clay concentration  $0.0625 \text{ g L}^{-1}$ , pH 7, and humic-acid concentrations indicated in the figure).

blanket is therefore not always beneficial to particle clarification.

Based on the solid-flux data, the three-dimensional solid-flux plot was constructed, characterized by the critical velocity and the upflow velocity at maximum solid flux. The critical velocity presented a plane in the figure, to the left of which the blanket could not stably exist. Based on fixed PACl dosage, the iso-humic-acid solid-flux surfaces stacked that enveloped the feasible regime for the blanket. The steady-state point moved toward low solid-flux and low solid-fraction regime with decreasing initial raw water turbidity and/or increasing humic-acid concentration. The present study revealed that the blanket concentration is a strong function of raw water turbidity and humic-acid concentration, and is not an adequate performance index subjected to a wide range of raw water quality.

The blanket produced by coagulation of low-turbidity raw water had large flocs when 1-ppm humic acid was present. This blanket also showed the best particle clarification efficiency compared with those without or with higher humic acid. There existed an optimal range of humic acid, approximately  $1 \text{ mg l}^{-1}$  in the present suspension, to yield a blanket that had strong structural strength to resist erosion under shear, and also had satisfactory particle clarification efficiency.

## Acknowledgments

The National Science Council, ROC, financially supported this work.

## References

- Annadurai, G., Sung, S.S., Lee, D.J., 2003. Floc characteristics and removal of turbidity and humic acid from high turbidity stormwater. *J. Environ. Eng. ASCE* 129 (6), 571–575.
- AWWA/ASCE., 1990. *Water Treatment Plant Design*. McGraw-Hill, New York (Chapter 7).
- Chen, L.C., Sung, S.S., Lin, W.W., Lee, D.J., Huang, C., Juang, R.S., Chang, H.L., 2003. Observations of blanket characteristics in full-scale floc blanket clarifiers. *Water Sci. Technol.* 47 (1), 197–204.
- Chu, C.P., Lee, D.J., 2001. Solids fluxes in consolidating sediments. *J. Chinese Inst. Chem. Eng.* 32, 547–554.
- Chu, C.P., Ju, S.P., Lee, D.J., Mohanty, K.K., 2002a. Batch sedimentation of slurries: effects of initial concentrations. *J. Colloid Interf. Sci.* 245, 178–186.
- Chu, C.P., Ju, S.P., Lee, D.J., Tiller, F.M., Mohanty, K.K., Chang, Y.C., 2002b. Batch settling of flocculated clay slurry. *Ind. Eng. Chem. Res.* 41, 1227–1233.
- Could, B.W., 1974. Upflow clarifiers—flow flexibility related to concentrator size. *Effl. Water Treatment J.* 14 (11), 621–631.
- Dempsey, B.A., 1989. Reactions between fulvic acids and aluminum. In: Suffer, I.N., MacCarthy, P. (Eds.), *Aquatic Humic Substances: Influence on Fate and Treatment of Pollutants*. American Chemical Society, Washington, DC, pp. 409–424.
- Dempsey, B.A., Ganho, R.M., O'Melia, C.R., 1984. The coagulation of humic substances by means of aluminum salts. *J. Am. Water Works Assoc.* 76, 141–150.
- Edzwald, J.K., Ives, K.J., Janssens, J.G., McEwen, J.B., Wiesner, M.R., 1999. *Treatment Process Selection for Particle Removal*. AWWRF/IWSA, New York (Chapter 7).
- Gregory, R., 1979. Floc blanket clarification: an explanation of the mechanism of floc blanket sedimentation intended as an aid to plant design and operation. WRC, TD 751/G74, UK.
- Gregory, R., Head, R., Graham, N.J.D., 1996. Blanket solids concentration in floc blanket clarifiers. *Proceeding of the Gothenburg Symposium*, Edinburgh, UK.
- Head, R., Hart, J., Graham, N.J.D., 1997. Simulating the effect of blanket characteristics on the floc blanket clarification process. *Water Sci. Technol.* 36 (4), 77–82.
- Ives, K.J., 1968. Theory of operation of sludge blanket clarifier. *Proc. Inst. Civil Eng.* 39, 243–260.

- Kawamura, S., 1991. *Integrated Design of Water Treatment Facilities*. Wiley, New York.
- Masschelein, W.J., 1992. *Unit Processes in Drinking Water Treatment*. Marcel Dekker, New York.
- Narkis, N., Rebhun, M., 1990. Flocculation of fulvic acids–clay minerals suspension. Proc. 21st Annual Meeting of the Fine Particle Society, San Diego, USA, pp. 1–25.
- O'Melia, C.R., 1991. Practice, theory, and solid–liquid separation. *J. Water SRT-Aqua* 40, 371–379.
- O'Melia, C.R., 2004. Coagulant requirements in potable water treatment. Proceedings of the 10th International Drinking Water Conference. 1–2 June 2004, Taipei, Taiwan.
- Rebhun, M., 1990. Floc formation and breakup in continuous flora flocculation and in contact filtration. In: Hahn, H.H., Klute, R. (Eds.), *Chemical Water and Wastewater Treatment*. Springer, Berlin, pp. 117–126.
- Rebhun, M., Lurie, M., 1993. Control of organic matter by coagulation and floc separation. *Water Sci. Technol* 27 (11), 1–20.
- Stevenson, D.G., 1997. *Water Treatment Unit Process*. Imperial College Press.
- Su, C.T., Wu, R.M., Lee, D.J., 2004. Blanket dynamics of upflow suspended bed. *Water Res.* 38 (1), 89–96.
- Sung, S.S., Lin, W.W., Chen, L.C., Lee, D.J., 2003. Spatial instability of blanket in full-scale blanket clarifiers. *J. Chinese Inst. Chem. Engrs.* 34 (4), 447–456.
- Tambo, N., Watanabe, Y., 1979. Physical characteristics of flocs. I: the floc density function and aluminum floc. *Water Res.* 13, 409–419.